PAPER *Special Section on Digital Signal Processing*

# ECG Data Compression by Matching Pursuits with Multiscale Atoms

**Makoto NAKASHIZUKA**[†a)], **Kazuki NIWA**[†], *and* **Hisakazu KIKUCHI**[††], ***Regular Members***

**SUMMARY** In this paper, we propose an ECG waveform compression technique based on the matching pursuit. The matching pursuit is an iterative non-orthogonal signal expansion technique. A signal is decomposed to atoms in a function dictionary. The constraint to the dictionary is only the over-completeness to signals. The function dictionary can be defined to be best match to the structure of the ECG waveform. In this paper, we introduce the multiscale analysis to the implementation of inner product computations between signals and atoms in the matching pursuit iteration. The computational cost can be reduced by utilization of the filter bank of the multiscale analysis. We show the waveform approximation capability of the matching pursuit with multiscale analysis. We show that a simple 4-tap integer filter bank is enough to the approximation and compression of ECG waveforms. In ECG waveform compression, we apply the error feed-back procedure to the matching pursuit iteration to reduce the norm of the approximation error. Finally, actual ECG waveform compression by the proposed method are demonstrated. The proposed method achieve the compression by the factor 10 to 30. The compression ratio given by the proposed method is higher than the orthogonal wavelet transform coding in the range of the reconstruction precision lower than 9% in PRD.

***key words:*** *multiscale analysis, matching pursuits, data compression, electrocardiogram, bio-medical signal processing*

## 1. Introduction

Electrocardiogram (ECG) is generated by the ambulatory measurement for the medical diagnosis of heart diseases. In ambulatory measurement, record samples are more than 10 millions a day. The amount of ECG data is so large that data compression and coding techniques are required for transmission and storage. Many ECG data compression techniques are proposed to record the huge size of ECG waveforms.

Previous ECG data compression techniques can be divided into two groups: direct methods and transform methods [1]. Direct methods are realized by irregular sampling and quantization of original waveforms in the time-domain. Transform methods are based on orthogonal transforms such as Fourier, KL, DCT [1] or wavelets [2]–[5]. Recently, the orthogonal wavelet transform is employed to ECG data compression. The wavelet transform can achieve high compression ratio by its time-frequency localization capability.

By the way, the matching pursuit that is a non-orthogonal signal expansion technique has been proposed [7]. A signal is decomposed to atoms that are included in a function dictionary. For matching pursuit signal decomposition, it is not necessary that each atom is orthogonal to others. The dictionary hence can be defined to best match the signal structure. It is expected that the frequency and time localization capability of the matching pursuit can be superior to orthogonal transforms. By this property, the matching pursuit has been already applied to low-bit rate video coding [9] and coding of prediction error in video coding [10]. In this paper, we applied the matching pursuit to ECG waveform compression and coding. In ECG waveform, a few sharp peaks appear during one heart-beat period. It is expected that a small number of atoms can approximate the ECG waveforms. Moreover, the matching pursuit algorithm includes both the signal expansion and reconstruction procedure. Hence, the iterative procedure guarantees the desired signal quality. Since the decoded signal can be obtained in the encoding process, we can get the coding residual between the decoded signal and the original signal. So, it is expected that the lossless compression can be easily achieved by the coding of residual signals.

The matching pursuit is realized by iterative procedures. An operation of the iteration consists of three steps: (1) Computation of inner products between the signal and all of atoms in the dictionary, (2) Search of the best atom that minimizes approximation error and (3) Computation of the approximation residual signal for the next iteration. The computation of inner products between all of the atoms in the dictionary is always required for every iteration. The computational cost of the matching pursuit hence is larger than orthogonal transforms. In this paper, we introduce the multiscale analysis and its filter bank structure to the computation of inner products to reduce the computational cost. The multiscale analysis can be implemented by the filter bank structure. The computational cost for inner products and approximation of the original signal for an iteration corresponds to a pair of analysis and reconstruction filtering.

In the next section, we give a brief explanation about previous works of the ECG data compression.

Manuscript received December 1, 2000.

Manuscript revised March 5, 2001.

[†]The authors are with the Graduate School of Bio-application and systems engineering, Tokyo University of Agriculture and Technology, Koganei-shi, 184-0012 Japan.

[††]The author is with the Faculty of Engineering, Niigata University, Niigata-shi, 950-2181 Japan.

a) E-mail: nkszk@cc.tuat.ac.jp

In Sect. 3, we explain the matching pursuit signal decomposition. Multiscale analysis is also introduced to the computation of the matching pursuit. We employ a 4-tap filter for the multiscale analysis for ECG approximation. The approximation of ECG waveforms will be also shown. In Sect. 5, the iteration of the matching pursuit for ECG waveform compression is discussed. In coding application, the coefficients of each atom are quantized. So, we introduce the error feed-back to the matching pursuit for reduction in the quantization error. Finally, the coding experiments for MIT/BIH database will be demonstrated.

## 2. Previous Works on the ECG Waveform Compression

A typical ECG waveform is shown in Fig. 1. One period of ECG waveform includes five transient waves that are called as P, Q, R, S and T wave. Sharp changes of the amplitude appear mainly around R waves. By contrast, P and T waves tend to appear as slow changes in amplitude. A few sharp peaks occur during a heart beat. The main problem of the ECG compression is to preserve the sharp amplitude variation that is important for the medical diagnosis while maintaining a high compression ratio.

ECG waveform compression methods that have been proposed can be divided into two categories, direct methods and the transform methods [1]. In direct methods, data reduction is achieved in the time domain. Classical direct methods are based on the adaptive sampling and quantization of the ECG samples. Recently, the improvement in DSP and computer systems allow more complex ECG compression techniques. Transform methods that are widely applied to image compression are also developed for ECG compression. Orthogonal transforms which are adopted to the image compression are also applied to ECG data compression. Recently, Orthogonal and biorthogonal wavelet transforms are mainly employed to ECG data compression [2]–[5]. In wavelet transform coding, the entire ECG waveform is divided to segments consisting of thousands samples. The orthogonal or biorthogonal wavelet transform is applied to each segment. After the transform, transform coefficients are quantized by the bit-allocation techniques to minimize the bit budgets [3]–[5]. The quantization of transform coefficients causes distortions which can appear in the form of irregular overdamped oscillation around discontinuities such as turning points that include peaks, start and stop points of the five transient waves that are important for medical diagnosis. One of the issues involved with the wavelet transform coding is better selection of the wavelet basis to reduce the distortions.

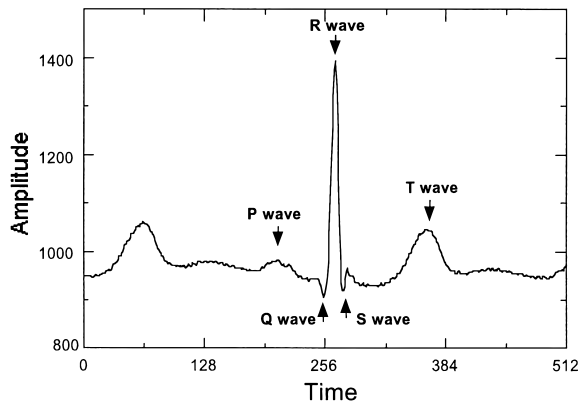


**Fig. 1** Typical ECG waveform.

In many studies of ECG compression, PRD (Percent Root Distance) has been employed as the measure of the reconstruction quality [1]. PRD is given by

$$PRD = \sqrt{\frac{\sum_{n=0}^{N-1}(x(n)-y(n))^2}{\sum_{n=0}^{N-1}x(n)^2}} \quad (1)$$

where $x(n)$ and $y(n)$ indicate the original and reconstructed signal, respectively. $N$ denotes the number of samples. PRD corresponds to the ratio between the squared sum of the reconstruction error and the squared sum of the original samples. In this paper, we also employ the measure to evaluate the quality of decoded waveforms.

## 3. Matching Pursuits with Multiscale Analysis

### 3.1 Matching Pursuits

In matching pursuits [7], a discrete signal $f(n)$ is approximated by the linear combination of atoms $\{q_\gamma(n)\}_{\gamma\in\Gamma}$ in a set of functions $D$ that is referred to as the dictionary. $\gamma$ denotes the index of atoms, and consists of a set of integers. Each integer specifies the properties of an atom, for example, scale, frequency or position. $\Gamma$ denotes the entire set of indices in a dictionary. The squared norm of an atom in the dictionary is normalized to unity.

An original signal $f(n)$ is approximated by those atoms as

$$f_M(n) = \sum_{i=0}^{M-1} P^{(i)} q_{\gamma_i}(n) \quad (2)$$

where $f_M(n)$ is the approximation. $M$ is the number of atoms. $\gamma_i$ is the index for the atom that is selected to approximate the original waveform. Atoms are selected by the following iterations. The initial approximation residual $R^{(0)}(n)$ is set as the original signal itself. At $i$-th iteration, inner products between all of atoms in a dictionary

$$P_{\gamma}^{(i)} = \langle R^{(i)}(n), q_{\gamma}(n) \rangle \tag{3}$$

are computed. The inner product which has the largest absolute is recorded as $P^{(i)}$ and its index of the atom $\gamma$ is recorded as $\gamma_i$. The approximation residual for the next iteration is defined by

$$R^{(i+1)}(n) = R^{(i)}(n) - P^{(i)} q_{\gamma_i}(n). \tag{4}$$

By the definition, the approximation residual $R^{(i+1)}(n)$ is orthogonal to the $i$-th atom $\gamma_i(n)$. By this iteration, a sequence of atoms that minimize the squared norm of successive residual $|R^{(i)}(n)|$ are selected. After $M$ iterations, the signal $f(n)$ is represented by a sequence of indices of atoms $\{\gamma_i\}_{0 \le i < M}$ and a sequence of coefficients $\{P_i\}_{0 \le i < M}$. Just a single constraint for a dictionary is that the dictionary is defined as over-complete basis to signals. If an original signal consists of $N$ samples, the number of atoms has to be larger than $N$. The dictionary has to involve set of $N$ atoms of which each atom is linearly independent to the other $N-1$ atoms. Thank to the freedom in selecting atoms, atoms can be chosen to best match the signal structure. If the dictionary is defined appropriately for an input signal, small $M$ is enough to its approximation. In matching pursuit iteration, the computation of inner products is required for all atoms that are not selected. The computational cost increases with the number of atoms in the dictionary. To reduce the computational cost for inner products, we introduce the multiscale analysis to generate the dictionary and to compute inner products in matching pursuits.

### 3.2 Atom Generation by the Multiscale Analysis

If the inner products computation of the matching pursuit is implemented by the direct convolution such as FIR filters, the computational cost is too huge to implement real time signal processing. By the way, the cascade connection of discrete filters, well known as filter banks can implement the convolution between various types of impulse responses and signals in simple structures. In this subsection, we employ a filter bank structure for the inner product computation between residual signals $R^{(i)}(n)$ and atoms. Figure 2 shows the basic filter bank structure which produces inner products between two types of the atoms and the input signal simultaneously.

In Fig. 2, $H(z)$ and $G(z)$ denote the Z-transform of the impulse responses $h(n)$ and $g(n)$ of two discrete-time filters. The filter bank gives the inner products

$$W_{(m)}^{(i)} = \left\langle \frac{1}{a} h_{(m)}(n), R^{(i)}(n) \right\rangle \tag{5}$$

and

$$S_{(m)}^{(i)} = \left\langle \frac{1}{b} g_{(m)}(n), R^{(i)}(n) \right\rangle \tag{6}$$

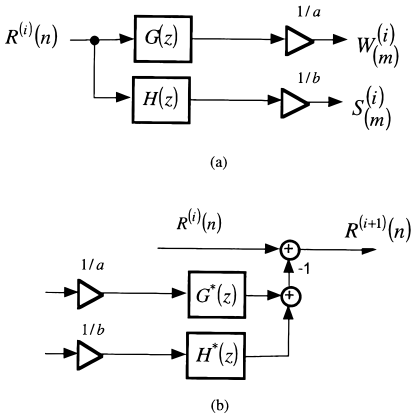


**Fig. 2** Basic structure of a two-band filter bank.

where $a$ and $b$ are constants for normalization of norm of atoms. The atoms $h_{(m)}(n)$ and $g_{(m)}(n)$ are the translation of $h(-n)$ and $g(-n)$ by $m$ and are identical to $h(-n+m)$ and $g(-n+m)$, respectively. In this case, we get a dictionary which consists of translation of atoms $g(-n)$ or $h(-n)$. So, atoms are defined as $q_{(m,1)}(n) = \frac{1}{a} h_{(m)}(n)$ and $q_{(m,2)}(n) = \frac{1}{b} g_{(m)}(n)$. The index $\gamma$ consists of two parameters, translation $m$ and an integer that specifies the filter. Inner products are also defined as $P_{(m,1)}^{(i)} = W_{(m)}^{(i)}$ and $P_{(m,2)}^{(i)} = S_{(m)}^{(i)}$. The filter output which has maximum absolute value is defined as the $i$-th coefficient for the matching pursuit approximation in Eq. (2). The dictionary implemented by Fig. 2(a) contains those atoms of which number is equal to twice the number of the signal samples.

Obviously, if there exists any sequences $k(n)$ and $l(n)$ of which Z-transforms $K(z)$ and $L(z)$ satisfy following equation:

$$H(z)K(z) + G(z)L(z) = 1 \tag{7}$$

then the dictionary satisfies the completeness condition. Usually, two-sequences $K(z)$ and $L(z)$ are defined in a synthesis filter bank. However, the matching pursuit requires only the conjugate filter $H^*(z)$ and $G^*(z)$ of which impulse responses are $h(-n)$ and $g(-n)$ are required for reconstruction. The existence of $K(z)$ and $L(z)$ is only required for the guarantee of the completeness of a dictionary. Figure 2(b) shows the filter bank structure for computation of the approximation residual for the next iteration. In Fig. 2(b), the filter inputs are defined as sequences that consist of impulses of which amplitude and positions are specified by the coefficients and indices.

Next, the cascade connection of filter banks is applied to get various length of atoms. In this paper, we apply the following two constraints to the set of atoms for approximation of ECG.

**1)** All atoms are symmetric and have a single peak with a small number of zero-crossings.
**2)** All atoms are generated by scaling and translation of a basic atom.

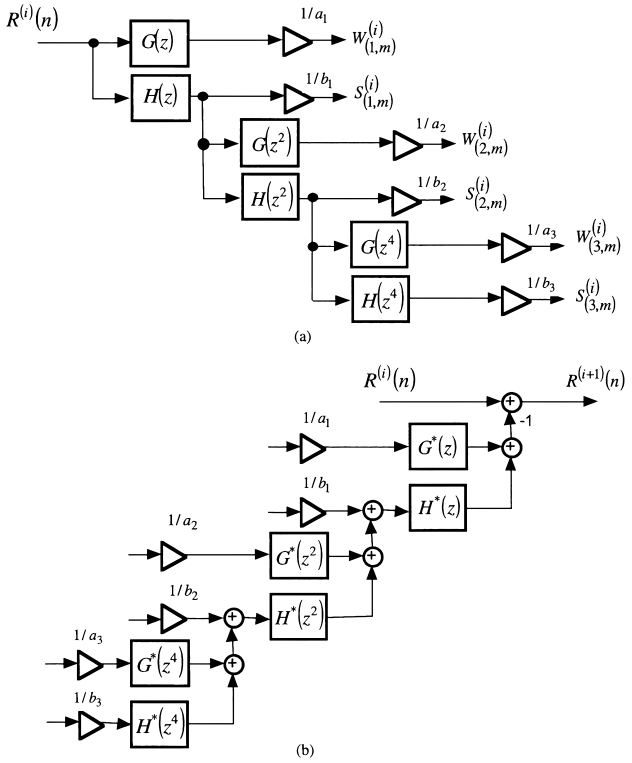


**Fig. 3** (a) Filter bank structure for computating inner products and (b) inverse filter bank for the approximation residual.

Each transient wave that compose ECG waveforms can be approximated by a function that has only one peak. We applied above the first constraint to approximate an individual transient wave by a single or a few number of atoms without the irregular fluctuations of the amplitude around peaks in reconstructed signals. Moreover, duration of Q, R and S waves is short and will be approximated by atoms at smaller scales. Contrary, duration of T and P waves is long and will be match to the atoms at larger scales. So, we define the entire dictionary by scaling and translation.

To satisfy the above two conditions, we apply the filter bank structure for multiscale analysis [6] which is shown in Fig. 3(a). Figure 3(b) shows a filter bank for the computation of the residual for next iteration. By this filter bank structure, we have two inner products

$$W^{(i)}_{(j,m)} = \left\langle \frac{1}{a_j} h_j(-n+m), R^{(i)}(n) \right\rangle \tag{8}$$

and

$$S^{(i)}_{(j,m)} = \left\langle \frac{1}{b_j} g_j(-n+m), R^{(i)}(n) \right\rangle \tag{9}$$

where $j$ denotes the scale index and is smaller than or equal to $J$. $J$ is the number of cascade connections of the filter. The constants $a_j$ and $b_j$ are required for normalization of atoms. Atoms which are given from the filter bank output are computed as

$$h_{j+1}(n) = \sum_k h(k) h_j(n - 2^j k) \tag{10}$$

and

$$g_{j+1}(n) = \sum_k g(k) h_j(n - 2^j k) \tag{11}$$

from $h_0(n)$ that is identical to a discrete-time delta function. The atoms are now defined as $q_{(j,m,1)}(n) = \frac{1}{a_j} h_j(-n+m)$ and $q_{(j,m,2)}(n) = \frac{1}{b_j} g_j(-n+m)$. The index $\gamma$ consists three parameters, scale $j$, translation $m$ and an integer that specifies the filter. Inner products are also defined as $P^{(i)}_{(j,m,1)} = W^{(i)}_{(j,m)}$ and $P^{(i)}_{(j,m,2)} = S^{(i)}_{(j,m)}$.

To satisfy above two condition, we apply the condition of the multiscale analysis to the sequence $h(n)$. The multiscale analysis [6] is defined by the inner products between the signal $f(x)$ and the scaling function $\phi_j(x)$ as:

$$S_j f(x) = \langle \phi_j(t-x), f(t) \rangle \tag{12}$$

where $\phi_j(x)$ denotes the scaling function at scale $2^j$ and is given by the dilation from the scaling function $\phi(x)$ as

$$\phi_j(x) = \frac{1}{2^j} \psi\left(\frac{x}{2^j}\right). \tag{13}$$

So, the multiscale analysis realizes the inner products between a signal and a set of similar functions. Usually, the scaling function is defined as a smoothing function. The multiscale analysis hence gives a set of smoothed signals in various scales. However, a discrete signal is defined on discrete points. So, a relationship between a continuous signal and a given discrete signal is assumed to exist. The assumption is such that a given discrete signal is the sampled smoothed signal at $j = 0$. The discrete signal is thus defined by $Sf_0(n)$. Moreover, let us assume that the scaling function $\phi(x)$ satisfies the two-scale relation as follows:

$$\phi_1(x) = \sum_k h(k) \phi_0(x-k). \tag{14}$$

By this assumption, the scaling function at scale index $j+1$ can be defined by the linear combination of the scaling function at $j$-th scale as

$$\phi_{i+1}(x) = \sum_k h(k) \phi_i(x - 2^i k). \tag{15}$$

By the assumptions with respect to the scaling function, the smoothed signal at scale index $j+1$ is represented by

$$Sf_{j+1}(n) = \sum_k h(k) Sf_j(n - 2^j k). \tag{16}$$

We define the filter in Fig. 2(a) to satisfy the condition Eq. (14) for any scaling function. So, outputs of the filter bank correspond to the inner products between the signal and scaling functions at various scales. The

**Table 1** Filter coefficients for filter banks.

| $n$ | $h(n)$ | $g(n)$ |
|---|---|---|
| -1 | 1/8 | 0 |
| 0 | 3/8 | 1 |
| 1 | 3/8 | 0 |
| 2 | 1/8 | 0 |

filter coefficients $h(n)$ that satisfy for any scaling function gives almost similar-looking atoms at any scale $j$. $g_j(n)$ is defined as a linear combination of $h_{j-1}(n-m)$. Set of $g_j(n)$ are also similar.

Next, approximation examples by the matching pursuit with filter banks are now demonstrated. The sequence of coefficients $h(n)$ that is employed to ECG approximation is shown in Table 1. This sequence is selected from the class of scaling functions which are obtained by cardinal B-spline [8]. The matching pursuit requires many number of iterations. So, we select a symmetric scaling function for cardinal B-spline wavelet which can be implemented with integer arithmetic computations. The order of the cardinal B-spline function is selected as second-order by experiments that are discussed in Appendix. To examine the signal approximation by only multiscale analysis, the sequence $g(n)$ is set as the discrete delta function. So, the inner products $W^{(i)}_{(j,m)}$ corresponds to $S^{(i)}_{(j-1,m)}$. The dictionary includes translated discrete-time delta functions and scaling functions. The number of cascade connections of the basic filter is set as seven. The total number of atoms in the dictionary is 8 times as the number of the original samples.

Example of the ECG waveform approximation in $M$=1, 16 and 32 are shown in Fig. 4, where $M$ is the number of atoms. In the approximation by a single atom, only the R wave that is most significant is reconstructed. The reconstruction quality increases as the number of atoms increases. Other transient waves of which amplitude is usually smaller than the R wave are reconstructed with 16 atoms. Fine details and the location of turning points are well preserved by using 32 atoms. The entire 512-sample waveform is well approximated with several atoms of which number is about 1/16 of the original samples with the signal precision in PRD 5%. The distribution of the atoms in the index plane is shown in Fig. 5. In this figure, the locations and heights of vertical bars indicates the position of the atoms and amplitude of the coefficients of those atoms. The position indices of atoms exactly indicate the positions of peaks of five kinds of transient waves of which correct positions are explicitly given in the entire waveform.

In this experiments, atoms are defined for all possible positions. Hence, the decomposition result has

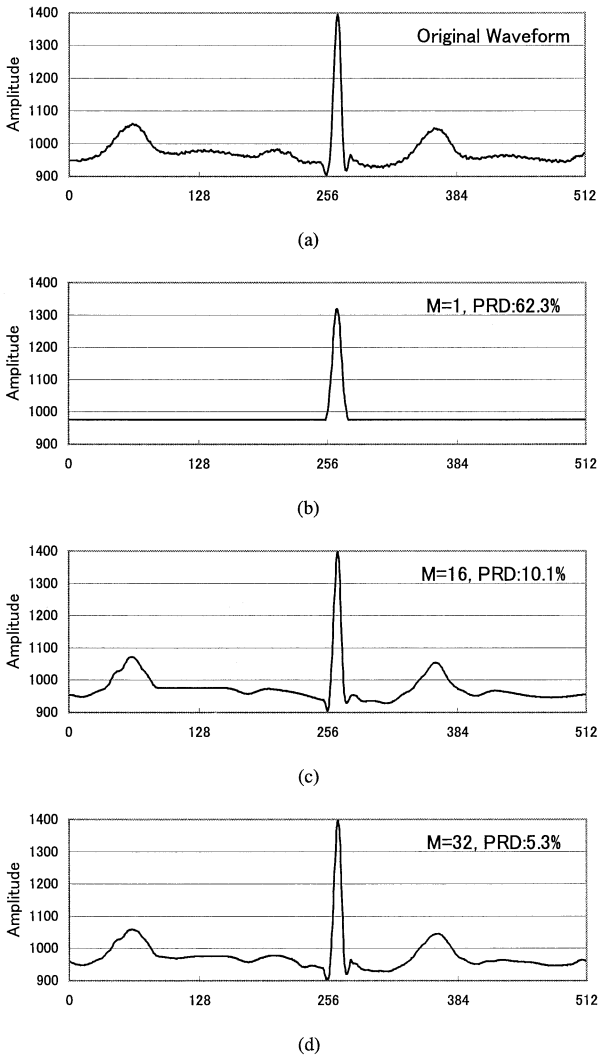


**Fig. 4** Approximation results by translation-invariant dictionary. (a) Original waveform, (b) approximation with a single atom, (c) 16 atoms and (d) 32 atoms.

translation invariant property. If the signal is translated in the time domain, the positions of atoms that are to be used for representing the translated signal are also translated. So, this dictionary can be referred as a translation-invariant dictionary. The computational cost for all atoms is equal in all scales. In larger scales, a short distance translation of signal causes just a little change in coefficient amplitude. So, we apply the decimation to the filter bank in Fig. 2(a) to reduce the number of atoms for signal decomposition. Figure 6 shows the filter bank structure with decimation. The dictionary is referred as a decimated dictionary. In Fig. 6, the number of atoms at $j$-th scale is decimated by factor $2^{j-1}$. So, the number of atoms is

$$N_D = N + \sum_{j=1}^{J} 2^{-j+1} N \tag{17}$$

where $N$ is the number of input samples and is now

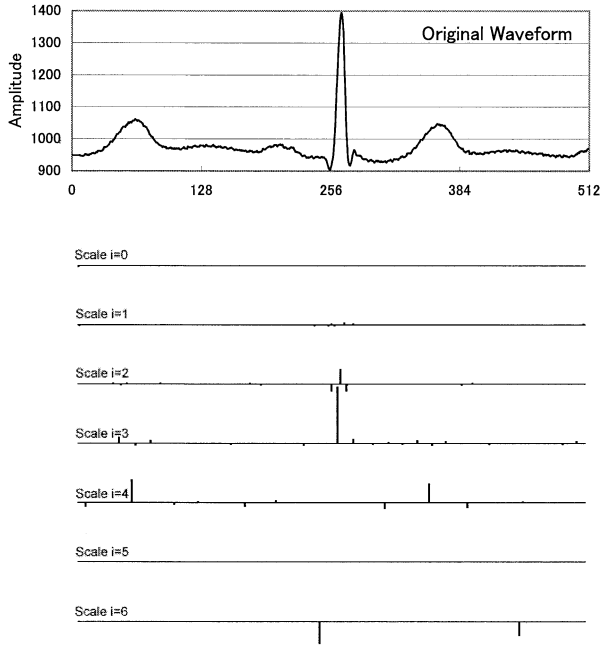


**Fig. 5** Location and amplitude of the multiscale in the scale-translation index plane.

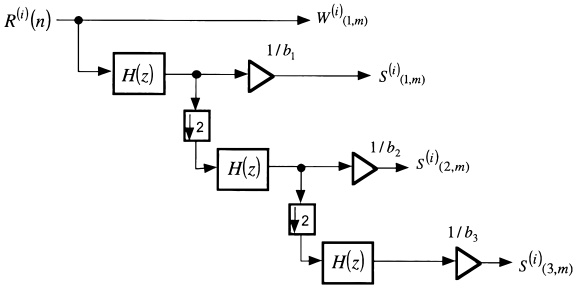


**Fig. 6** Filter bank structure for multiscale atoms with decimation. ($J = 3$)

supposed to the power of two. $J$ is set as an integer which satisfies $2^{J-1} \leq N$. So, $N_D$ is smaller than triple as many as input samples. In the translation-invariant dictionary with the filter coefficients in Table 1, the number of atoms is

$$N_T = (J + 1)N. \tag{18}$$

In the experiments, the number of atoms in translation-invariant dictionary is 4,096 atoms for 512 input samples. The decimated dictionary consists of 1,528 atoms. The approximation results by the decimated dictionary are shown in Fig. 7. The approximation precision is slightly lower than the translation-invariant dictionary. The approximation precision is shown in Fig. 8 for two dictionaries. Obviously, the translation-invariant dictionary that contains a larger number of atoms achieves higher approximation precision. The decimated dictionary requires more atoms to achieve the same approximation precision obtained by the translation-invariant dictionary.

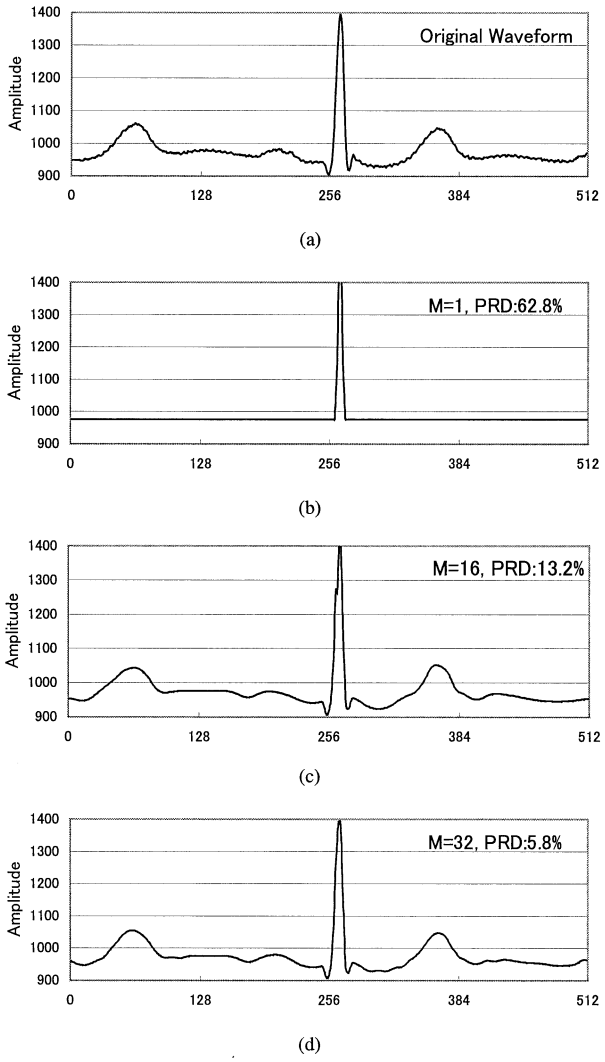


**Fig. 7** Approximation results by decimated dictionary. (a) Original waveform, (b) approximation with a single atom, (c) 16 atoms and (d) 32 atoms.

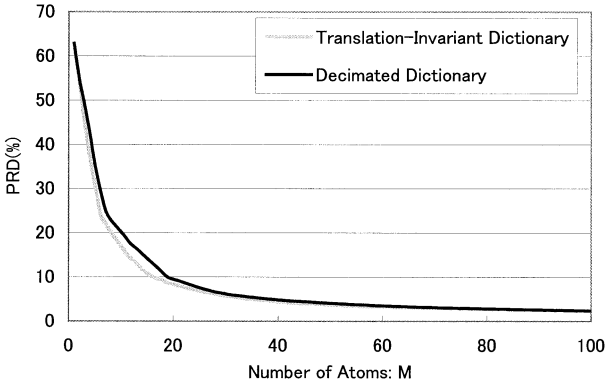


**Fig. 8** Approximation precision in PRD.

## 4. Iterative Procedure for Waveform Compression

The signal waveform is represented by two sequences

of indices and coefficients of atoms. In actual coding systems, the inner products have to be quantized. In addition, the signal reconstruction process can be included in the decomposition process in the matching pursuit iteration. So, the quantization error can be acounted into the approximation residual that is the target waveform in the next approximation step. The computational of residual in Eq. (4) is represented by:

$$R^{(i+1)}(n) = f(n) - \sum_{k=1}^{i} P^{(k)} q_{\gamma_k}(n). \tag{19}$$

The individual second term of the right side-hand corresponds to a signal reconstruction from the indices and inner products. If the signal reconstruction process in Eq. (19) includes the quantization, $R^{(i+1)}(n)$ includes both of the approximation residual and the quantization error. The $i+1$-th iteration decreases the both the approximation residual and the quantization error that causes at $i$-th iteration. Now, the quantization of the coefficients is denoted as $Q[\cdot]$. By inserting the quantization to Eq. (19), we can get

$$R^{(i+1)}(n) = f(n) - \sum_{k=1}^{i} Q[P^{(k)}] q_{\gamma_k}(n). \tag{20}$$

The approximation residual converges when $Q[P^{(i)}]$ shrinks to zero. If the quantization is realized by rounding with the uniform quantization step $\delta$, the iteration converges when the all inner products are smaller than the $\delta/2$. In the case of the atoms that are generated from the filter coefficients in Table 1, the approximation residual

$$|R^{(i+1)}(n)| < \delta/2 \tag{21}$$

when the iteration converges. So, the upper bound of the squared norm of the residual $R_i(n)$ depends on the quantizing step $\delta$ and is estimated as $N\delta^2/4$ where $N$ is the number of samples of the original signal. Figure 9 shows the relationship between the number of iterations and the approximation error in terms of root of mean squared error. The upper bound of the error is given by a half of $\delta$. Figure 9 shows that RMSE at convergence decreases as $\delta$.

Next, we explain the iteration process. In actual ECG coding, only finite number of iteration can be implemented. We suppose that the desired precision of the reconstructed signal and initial quantizing step $\delta$ are given before encoding. At first, the ECG waveforms are divided to the segment containing $N$ samples. The matching pursuit is applied to each segment individually. In the initial condition, the initial approximation residual $R^{(0)}(n)$ is set as the original ECG samples. The coefficients table for atoms are described as $s_{j,m}$ and $w_{j,m}$. All elements in $s_{j,m}$ and $w_{j,m}$ are set as zero. The total number of elements $s_{j,m}$ and $w_{j,m}$ corresponds to the number of atoms. Integers $j$ and

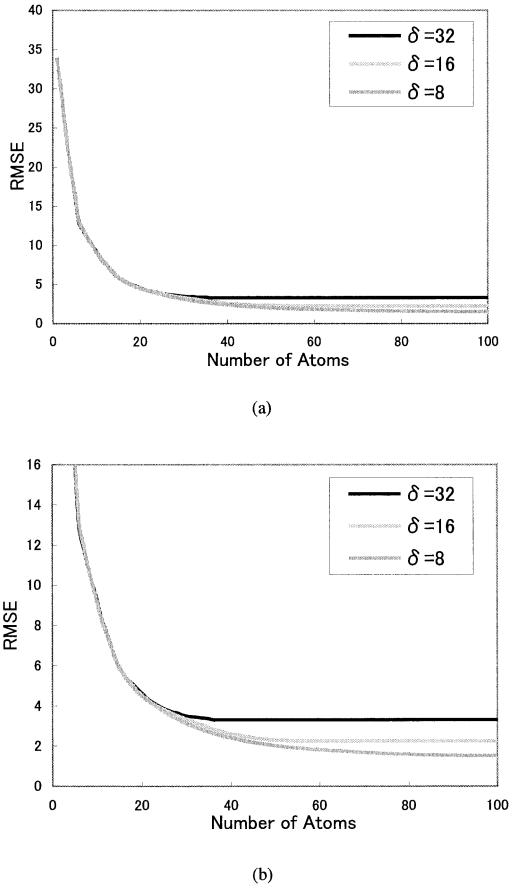


**Fig. 9** Relationship between quantization steps and approximation error. (Part(b) is the same with (a), but is magnified in the vertical scale)

$m$ indicate the scale and translation position of atoms, respectively. $\delta$ is the initial quantization step. The desired reconstruction precision is given in PRD. The matching pursuit iteration stops, when the reconstruction precision becomes lower than a given desired level. After the above initial conditions have been defined, the following iteration begins from $i = 0$.

**Step 1** Compute inner products of $R^{(i)}(n)$ by the filter bank given in Table 1.

**Step 2** Find the index $(j, m)$ that maximize the inner products. The found index is written by $(j_{max}, m_{max})$.

**Step 3** If the maximum inner product that is found in Step 2 is $W^{(i)}_{(j_{max},m_{max})}$, then update the table as

$$w_{j_{max},m_{max}} \leftarrow w_{j_{max},m_{max}} + Q[W^{(i)}_{(j_{max},m_{max})}]. \tag{22}$$

If the maximum inner product is $S^{(i)}_{(j_{max},m_{max})}$, then update the table as

$$s_{j_{max},m_{max}} \leftarrow s_{j_{max},m_{max}} + Q[S^{(i)}_{(j_{max},m_{max})}]. \tag{23}$$

**Table 2** Compression results for MIT103.

| Desired PRD(%) | | 15% | 13% | 11% | 9% | 7% |
|---|---|---|---|---|---|---|
| Compression Ratio | Proposed Method (with translation-invariant dictionary) | 29.5:1 | 25.8:1 | 22.5:1 | 17.8:1 | 13.9:1 |
| | Proposed Method (with decimated dictionary) | 32.31 | 26.2:1 | 25.1:1 | 20.0:1 | 16.4:1 |

where $Q[\cdot]$ denotes the quantization with step $\delta$.

**Step 4** Reconstruct signal from $s_{(j,n)}$ and $w_{(j,n)}$ by the inverse filter bank and compute the approximation residual $R_{i+1}(n)$. If approximation residual is lower than the desired precision, then stop the iteration. If the approximation precision is equal at the previous iteration, then $\delta$ is update to halved.

**Step 5** Go to Step 1.

In the above iteration, the maximum of the inner products is smaller than a given temporary quantization step, the approximation process will complete. If the approximation precision converges before the precision does not reach to the desired precision, the quantizing step is update to the half of the temporary quantization step. After the iteration, the segment of waveform is represented in the coefficients table $s_{j,m}$ and $w_{j,m}$ which involve non-zero elements of which number is equal to the number of the iteration.

Now let us discuss computational costs for the matching pursuit decomposition with the filter bank. $F$ is denoted as the number of the filter taps for $H(z)$ and $G(z)$. At first, the computational cost for an iteration of the matching pursuit is estimated. The pair of the analysis and synthesis filterbanks requires $4JFN$ and $2F(N_D - N)$ times pairs of multiplication and addiction for the translation-invariant dictionary in Fig. 3 and decimated dictionary in Fig. 6, respectively. For both dictionaries, the normalization operation requires multiplications as many as the number of atoms. To find the maximum amplitude atom, comparison operations are also required as many as the number of atoms. Moreover, $N$-times additions and subtractions are required for the computation of PRD for an iteration. The entire computational cost until convergence is equal to the product of the computational cost for an iteration by the number of iterations $M$.

Let suppose that the orthogonal wavelet filter bank is implemented by the pair of two $F$-tap filters to compare with the matching pursuit. $J$-th scale orthogonal wavelet transform requires $2F\sum_{j=0}^{J-1} 2^{-j}N$ times pairs of multiplication and addition that is less than $4FN$. The computational cost of the matching pursuit is about more than $JM$ and $M$ times of the orthogonal wavelet transform for the translation-invariant and the decimated dictionary, respectively. The disadvantage of the matching pursuit signal decomposition is that the redundant bases and the iteration requires huge amount of computational costs.

## 5. ECG Waveform Coding

Some coding examples by the matching pursuit with filter banks are now demonstrated. The filter coefficients that are shown in Table 1 are employed for signal decomposition. By these filter coefficients, $\{w_{1,m}\}$ and $\{s_{j,m}\}_{1\le j<J}$ comprise the atom elements table. We tested two types of ECG signals that include different features in MIT-BIH Arrhythmia Database. First is MIT200 tested in Ref. [5] for comparison between the orthogonal wavelet transform coding method that is proposed in Ref. [5]. The other is MIT103 that contains almost normal heart beats without heavy noises. Each record contains 216,000 samples produced by 360Hz sampling in 11-bit resolution.

The entire record is divided into coding segments contains $N = 1,024$ samples. A coding segment is approximated by the matching pursuit with the filter bank individually. The maximum scale index of the filter bank is set as seven. The number of atom pairs are $8,192$ for a translation-invariant dictionary and $3,056$ for a decimated dictionary.

By the iterative procedure in the previous section, each ECG segment is represented in the coefficients table. Only the indices $(j, n)$ that are selected during the iteration have non-zero coefficients. For coding the coefficients and indices, each index of the non-zero coefficient is converted to a single position index that is defined as $j \times N_j + m$ for $s_{j,m}$ and $m$ for $w_{1,m}$. $N_j$ denotes the number of atoms at $j$-th scale. The differences between two consecutive position indices are coded to record indices of atoms. Values of coefficients are also recorded along the position indices increases. The position differences and the value of coefficients that are given from all segments are encoded by the Huffman coding. The other components, the quantizing steps for each segments are also coded by the Huffman coding.

In coding experiments, we set the desired signal quality as 15, 13, 11, 9 and 7% in PRD. In Tables 2 and 3 show the compression ratio between the original and the compressed data. In compression results for MIT200, a wavelet transform coding reported in Ref. [5] is also referred. The wavelet transform coding results are given by the orthogonal wavelet of the Daubechies

**Table 3** Compression results for MIT200.

| Desired PRD(%) | | 15% | 13% | 10% | 9% | 7% |
|---|---|---|---|---|---|---|
| Compression Ratio | Proposed Method (with translation-invariant dictionary) | 24.9:1 | 21.3:1 | 17.8:1 | 14.0:1 | 10.4:1 |
| | Proposed Method (with decimated dictionary) | 28.2:1 | 24.1:1 | 20.1:1 | 16.1:1 | 12.2:1 |
| | Orthogonal Wavelet Transform Coding in Ref[5] | | 22.9:1 | | 16.0:1 | 12.5:1 |

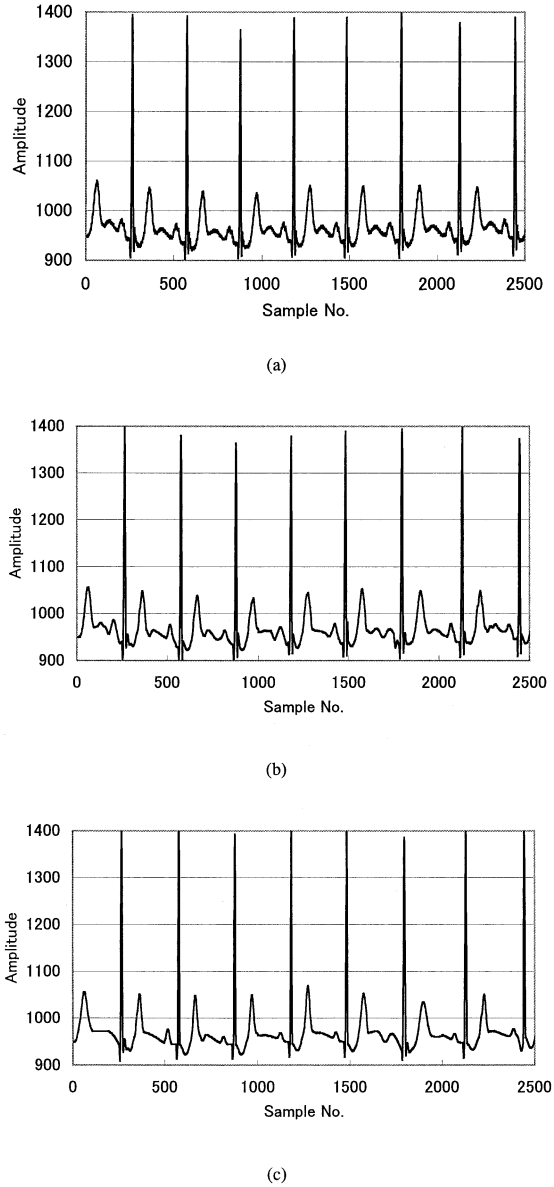


**Fig. 10** Reconstructed waveforms of MIT-BIH arrhythmia record 103 with translation-invariant atoms: (a) orginal ECG (b) reconstructed at PRD=7%, compression ratio 15.9:1 and (c) PRD=12.9%, compression ratio 30.0:1.

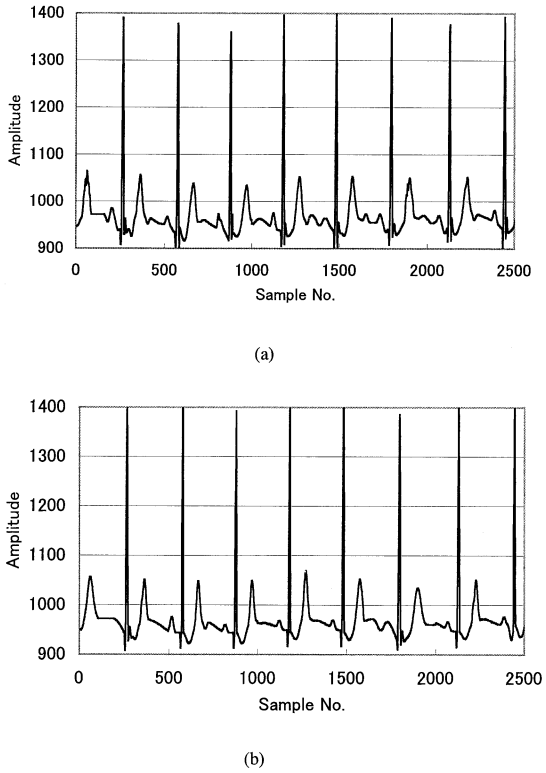


**Fig. 11** Reconstructed waveforms of MIT-BIH arrhythmia record 103 with decimated atoms: (a) reconstructed at PRD=7.0%, compression ratio 18.2:1 and (b) PRD=13.0%, compression ratio 31.9:1.

10-tap coefficients and an adaptive quantizer [5]. Comparison between the wavelet transform coding [5] and the proposed method with the decimated dictionary shows higher compression ratios beyond 9% in PRD. Obviously, code words for indices are not required for the transform coding. So, the matching pursuit is superior to the transform coding when a small number of atoms are enough for compression. In matching pursuits, the overhead of the index codes increases along the number of atoms increases. So, the compression ratio is slightly lower than the orthogonal transform in high quality compression.

The reconstructed waveforms are shown in Figs. 10 to 13. Figures 10 and 12 are the results by the translation-invariant dictionary. Figures 11 and 13 are

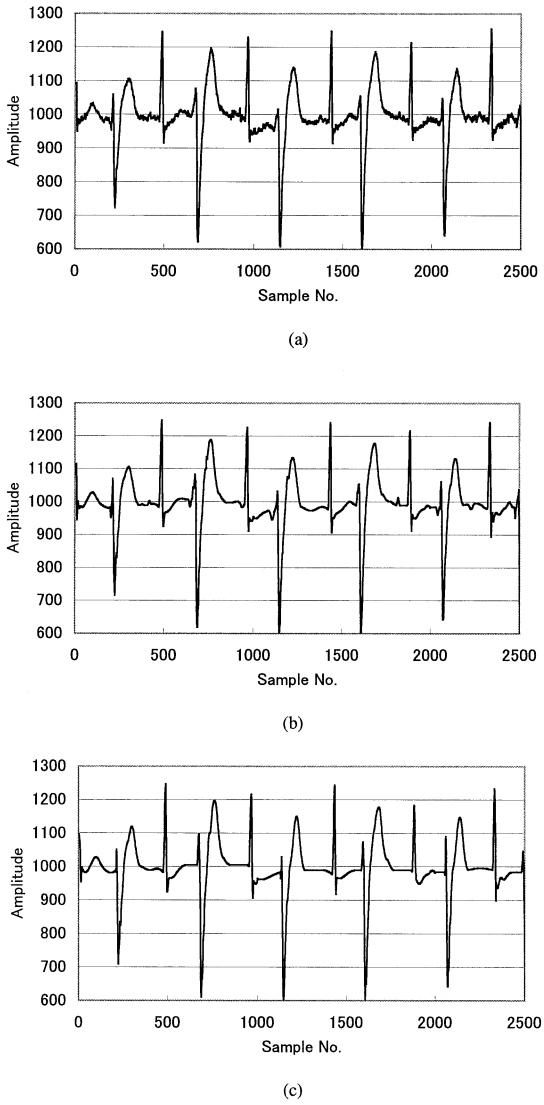


**Fig. 12** Reconstructed waveforms of MIT-BIH arrhythmia record 200 from translation-invariant atoms: (a) orginal ECG (b) reconstructed at PRD=7%, compression ratio 10.4:1 and (c) PRD=12.9%, compression ratio 21.3:1.

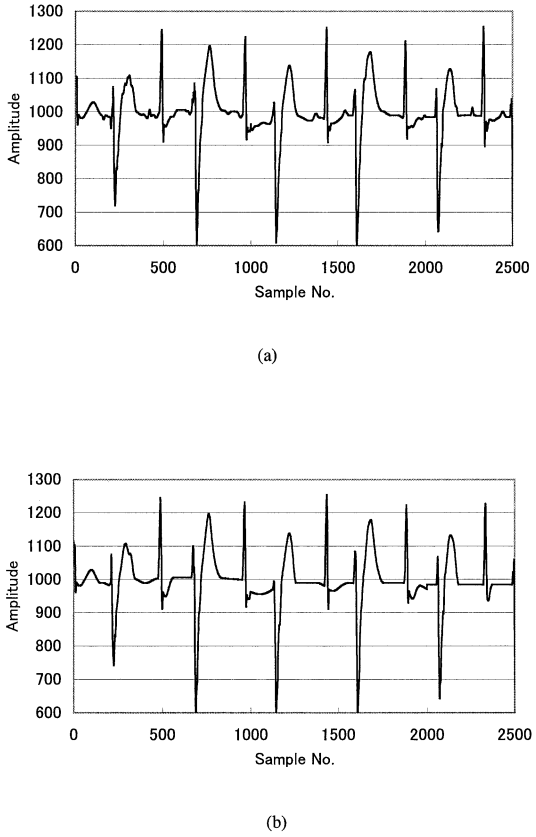


**Fig. 13** Reconstructed waveforms of MIT-BIH arrhythmia record 200 from decimated atoms: (a) reconstructed at PRD=7.0%, compression ratio 12.2: and (b) PRD=12.9%, compression ratio 24.1:1.

the results by the decimated dictionary. Figure 14 shows reconstructed waveforms from the wavelet transform coding with the Daubechies 10-tap coefficients and an adaptive quantizer [5]. Distortions and irregular oscillations appear around sharp variation points in the reconstruction waveform from the wavelet transform coding in Fig. 14. In contrast to the wavelet transform coding, artifacts do not occur in the reconstructed waveform by the proposed method. This reason is that the atoms of the proposed method correspond to the simple smoothing functions with no zero-crossings and are located to the positions of peaks of the transient waves. This property will be desirable for better diagnosis and precise measurement of time period around transient waves.

In Table 4, the average number of atoms for compression in each segment is shown. The decimated dictionary requires a larger number of atoms than the translation-invariant dictionary. About 30 to 50 atoms are required to a rough approximation. 70 or more atoms are required for a precise approximation. Table 5 shows the code amount for indices and coefficients of atoms for coding of MIT200. In the every compression results, 60% to 70% of the entire codes are spent for the recording indices of atoms. Since the number of atoms in the translation-invariant dictionary is larger than the decimated dictionary, the code amount for the indices of atoms that are required for the decimated dictionary is smaller than the translation-invariant dictionary. By contrast, the decimated dictionary requires lager number of atoms than the translation-invariant dictionary. So, the data amount for the coefficients of the decimated dictionary is larger than the translation-invariant dictionary.

Another demonstration is shown in Fig. 15. In this experiment, the noise reduction property of the proposed method and the wavelet transform coding are compared. One of major problems in ambulatory measurement of ECG is the presence of noises. Reference [7] reports that matching pursuits can achieve well noise reduction by its time-frequency localization capability.

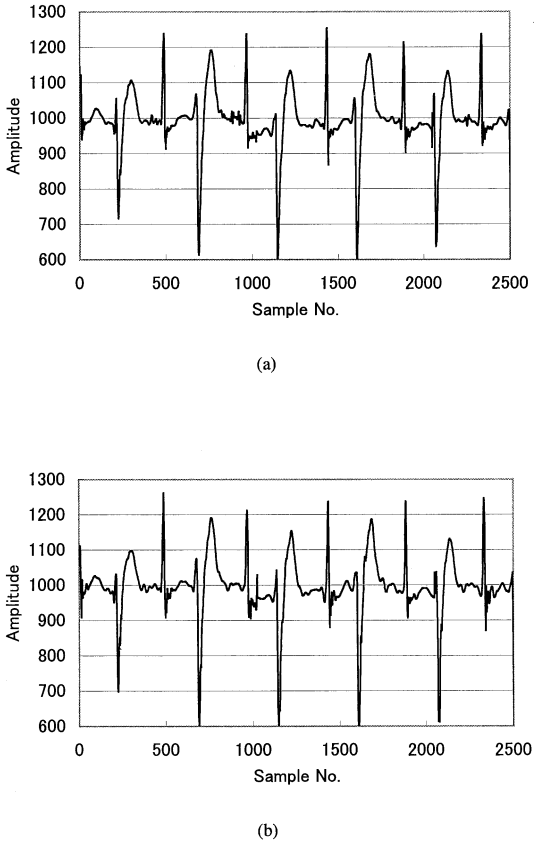


**Fig. 14** Reconstructed waveforms of MIT-BIH arrhythmia record 200 from orthogonal wavelet transform method (a) PRD=7% and (b) PRD=13%.

**Table 4** Average number of atoms in a coding segment.

| | | 15% | 13% | 11% | 9% | 7% |
|---|---|---|---|---|---|---|
| MIT200 | Translation-invariant | 29.6 | 36.9 | 47.5 | 65.0 | 95.8 |
| | Decimated | 32.1 | 40.0 | 51.4 | 70.1 | 100.9 |
| MIT103 | Translation-invariant | 26.9 | 31.7 | 38.6 | 51.1 | 72.0 |
| | Decimated | 28.1 | 33.5 | 41.0 | 55.3 | 75.5 |

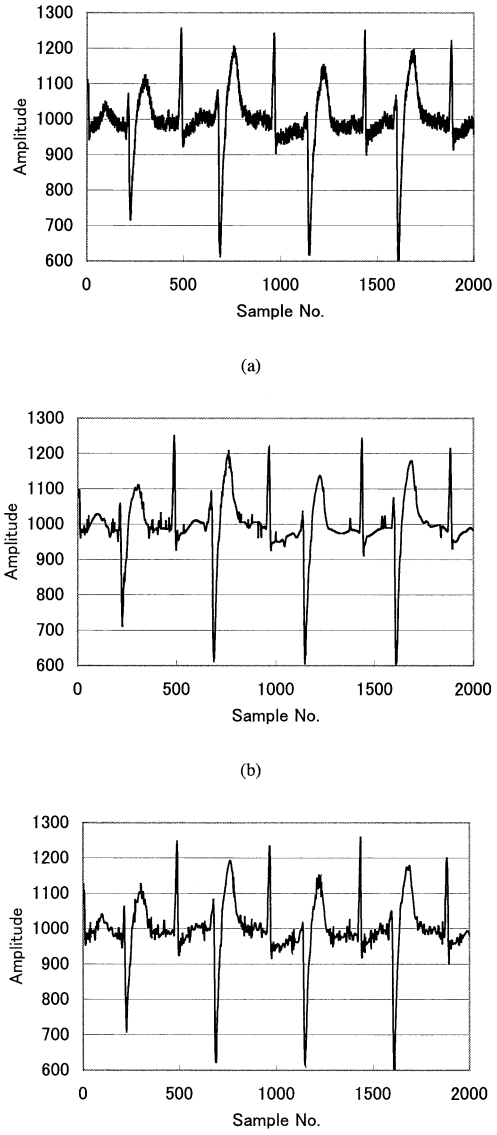


**Fig. 15** (a) ECG waveform corrupted random noise, (b) reconstructed waveform from matching pursuits at desired PRD=13% and (c) reconstructed waveform from wavelet transform coding at desired PRD=13%.

**Table 5** Data amount of each component for MIT200.

| | | 15% | 13% | 11% | 9% | 7% |
|---|---|---|---|---|---|---|
| translation-invariant Dictionary | Code Amount for atom indices (bytes) | 24,690 | 28,794 | 34,291 | 43,026 | 56,719 |
| | Code Amount for coefficients (bytes) | 9,914 | 11,763 | 14,438 | 19,075 | 27,032 |
| Decimated Dictionary | Code Amount for atom indices (bytes) | 19,696 | 22,976 | 27,396 | 33,948 | 43,702 |
| | Code Amount for coefficients (bytes) | 10,795 | 12,812 | 15,700 | 20,506 | 28,121 |

**Table 6** Noise reduction property of each coding method for segments in Fig. 15(a).

| Desired PRD(%) | 13% | | 7% | |
|---|---|---|---|---|
| MSE of input signal corrupted by random noise | 205.8 | 74.2 | 205.8 | 74.2 |
| MSE of reconsturucted signal (Matching pursuits with translation invariant dictionary) | 120.3 | 67.0 | 206.3 | 57.0 |
| MSE of reconsturucted signal (Matching pursuits with decimated dictionary) | 125.9 | 69.3 | 209.0 | 60.0 |
| MSE of reconsturucted signal (Wavelet Transform) | 209.6 | 72.5 | 252.4 | 94.0 |

We also examine the property of the noise reduction of the coding method and compare with the transform coding method. Figure 15(a) shows an ECG waveform corrupted with random white noise. MSE(Mean Squared Error) of the waveform segment in Fig. 15(a) is 205.8. Both the wavelet transform coding and the proposed coding method are applied to the corrupted signal. The reconstructed signals are shown in Fig. 15(b) from the proposed method with the decimated dictionary and Fig. 15(c) from the wavelet transform method. Desired PRD is set as 13% for both coding method. The approximation and quantization are done to satisfy that reconstruction error which is defined between the corrupted input signal and the reconstructed signal is smaller than the specified PRD. Comparing Fig. 15(b) to Fig. 15(c), the amplitude of noise in the reconstructed signal from the proposed method is smaller than noise in the wavelet transform method. In Table 6, MSE of reconstructed signals from both coding method at PRD 13% and 7% are shown. MSE of reconstructed signals from the proposed coding method are smaller than the wavelet transform coding method at every examples. These results show that the matching pursuit signal approximation has better waveform preservation property than the wavelet transform coding method. The matching pursuit isolates the signal structures that are coherent with respect to a given dictionary. The only main structures of the original signal can be retained quickly during iterations.

Finally, actual computational time for 30 minutes ECG records(MIT200) with the translation-invariant dictionary are shown in Table 7. This table shows the computational time for signal decomposition by the matching pursuit and the wavelet transform. The computational time for 30 minutes ECG is about 3 to 9 minutes by Pentium 166 MHz processor. Real time ECG compression will be archived by the proposed method by such a class of processors. However, the computational time of the proposed method is larger than about 200 times of the wavelet transform coding method.

**Table 7** Computation time for 30 minutes ECG record (running on Pentium 166 MHz Processor).

| | Comp. time (s) |
|---|---|
| Matching Pursuits (PRD=13%) | 197.3 |
| Matching Pursuits (PRD=7%) | 547.2 |
| Wavelet transform | 1.2 |

## 6. Conclusion

In this paper, an ECG waveform compression based on the matching pursuits. The filter bank structure was introduced to the matching pursuits to reduce the computational costs for the inner products computation. The error-feed back was introduce to the matching pursuit iteration to reduce the quantization error. 4-tap symmetric integer filter bank system has been enough to practical ECG compression and gives competitive or higher compression ratios than the orthogonal transform method [5]. The proposed method keeps primary features of waveforms and does not cause artifacts that can be caused by the quantization of the orthogonal transform coefficients. Owing to this property, the proposed method is suitable for low-bit rate ECG compression and transmission. Moreover, the indices of atoms in the translation-invariant dictionary exactly indicate the peaks of ECG. So, it is expected that the compressed data is also utilized to the computerized ECG diagnosis, such as feature detection.

The disadvantage of the proposed method is the computational cost for the iterative procedure. However, the compression results have shown that just 4 tap integer filter is enough to actual ECG compression. Moreover, one stage filter bank can be constructed by the single low-pass filter. Any bit-allocation technique is not required to achieve high compression ratio.

The matching pursuits permit any filter to be applied for signal decomposition, since its decomposition does not require orthogonal and bi-orthogonal properties. The optimum filter design for waveform coding is a future subject. In signal decomposition, the number of atom depends on a signal. For example, a noisy signal requires many atoms. While effective noise reduction is incorporated in the matching pursuits signal decomposition process, its optimization is also an open question.

## Acknowledgement

This work was in part supported by the research grant for operational information and telecommunication systems for sharing advanced medical resources given by Telecommunication Advancement Organization (TAO) of Japan.

### References

[1] S. Jalaleddine, C. Hutchens, R. Strattan, and W. Coberly, "ECG data compression techniques—A unified approach," IEEE Trans. Biomed. Eng., vol.37, no.4, pp.329–343, April 1990.
[2] N.V. Thakor, Y.C. Sun, H. Rix, and P. Caminal, "Multiwave: A wavelet-based ECG data compression algorithm," IEICE Trans. Inf. & Syst., vol.E76-D, no.12, Dec. 1993.
[3] A. Djohan, T.Q. Nguyen, and W.J. Tompkins, "ECG compression using discrete symmetric wavelet transform," Proc. 17th Annual International Conference of the IEEE Medical and Biology Society, Montral, Sept. 1995.
[4] G. Strang and T.Q. Nguyen, Wavelets and filter banks, Wellesley-Cambridge Press, 1997.
[5] J. Chen and S. Itoh, "A wavelet transform-based ECG compression method guaranteeing desired signal quality," IEEE Trans. Biomed. Eng., vol.45, no.12, pp.1414–1419, Dec. 1998.
[6] S. Mallat, "A theory for multiresolution signal decomposition: The wavelet representation," IEEE Trans. Pattern Anal. & Mach. Intell., vol.11, no.7, pp.674–693, July 1989.
[7] S. Mallat and Z. Zhang, "Matching pursuits with time-frequency dictionaries," IEEE Trans. Signal Processing, vol.41, no.12, pp.3397–3415, Dec. 1993.
[8] C.K. Chui, An introduction to wavelets, Academic Press, Orlando, 1992.
[9] R. Neff and A. Zakhor, "Very low bit-rate video coding based on matching pursuits," IEEE Trans. Circuits & Syst. for Video Tech., vol.7, no.1, pp.158–171, Feb. 1997.
[10] M.R. Banham and J.C. Brailean, "A selective update approach to matching pursuits video coding," IEEE Trans. Circuits & Syst. for Video Tech., vol.7, no.1, pp.119–129, Feb. 1997.

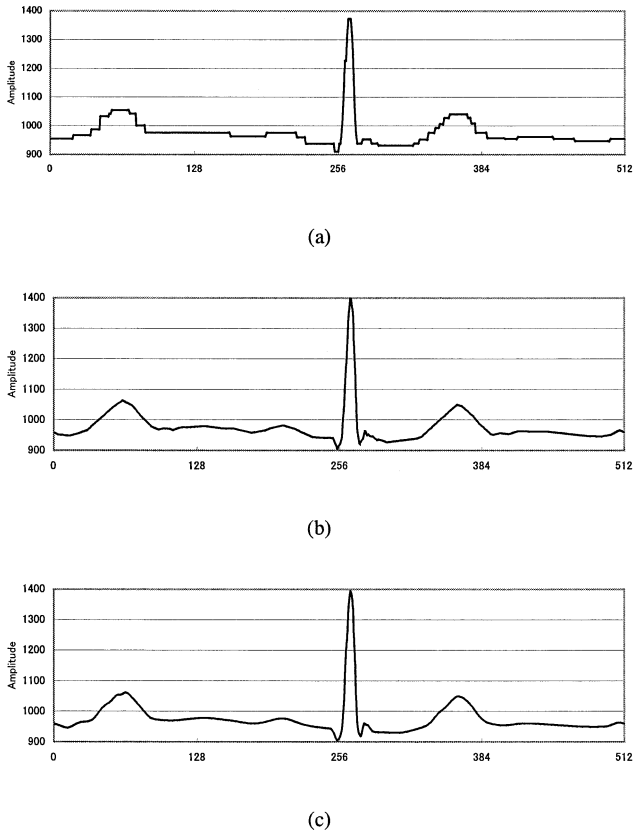


**Fig. A· 1** (a) Approximation results by zero-order spline functions (PRD: 11.5%), (b) first-order spline functions (PRD: 5.8%) and (c) third-order spline functions (PRD: 6.4%).

## Appendix: Examples of ECG Approximation by Cardinal B-Spline Scaling Functions

In cardinal B-spline wavelets [8], the order of the spline function specifies differentiability and regularity of the scaling function. We show the approximation results with scaling functions that are zero, first and third order cardinal B-spline function in Fig. A· 1. The number of atoms for approximation is set as 32. Comparing with Fig. 4 that is given by the second order cardinal B-spline, the lower order functions give less approximation precision or cause discontinuities in waveforms. The higher order function is too smoother to approximate sharp variation changes and gives lower approximation precision than second order function. We hence select the second order B-spline function for ECG waveform approximation and coding.

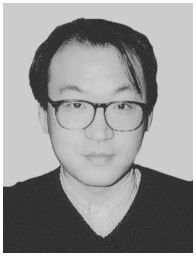

**Makoto Nakashizuka** was born in Niigata, Japan in 1966. He received B.E., M.E., and Ph.D. degrees from Niigata University, Niigata, Japan, in 1988, 1990, 1993. He was with Department of Information Engineering, Niigata University as a Research Associate from 1993 to 1997. He is now an Associate Professor at Graduate School of Bio-Applications and Systems Engineering, Tokyo University of Agriculture and Technology. His research interests include time-scale/frequency analysis and its applications to signal, bio-medical, image and vision processing. Dr. Nakashizuka is a member of IEEE, Institute of Image Information and Television Engineers and Japan Society of Medical Electronics and Biological Engineering.

**Kazuki Niwa** was born in Aichi, Japan in 1975. He received B.E. degree from Tokyo University of Agriculture and Technology, Tokyo, Japan, in 1998. He is now a master course students in Graduate School of Bio-Applications and Systems Engineering, Tokyo University of Agriculture and Technology. His research interests include digital signal processing, multiscale analysis and signal decomposition.

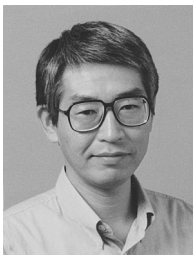

**Hisakazu Kikuchi** received B.E. and M.E. degrees from Niigata University, Niigata, Japan, in 1974 and 1976, respectively, and Dr.Eng. degree in electrical and electronic engineering from Tokyo Institute of Technology, Tokyo, Japan, in 1988. From 1976 to 1979 he worked at Information Processing Systems Laboratory, Fujitsu Ltd., Tokyo. Since 1979 he has been with Niigata University, where he is a Professor at Department of Electrical Engineering. During a year of 1992 to 1993, he was a visiting scientist at the Electrical Engineering Department, University of California, Los Angeles sponsored by the Ministry of Education, Science and Culture of Japan. His current research interests include digital signal processing, image/video processing, and wavelets as well as spread spectrum communication systems. Dr. Kikuchi is a member of Institute of Image Information and Television Engineers of Japan, and Japan Society for Industrial and Applied Mathematics, and IEEE.